

*[This manuscript has been authored by UT-Battelle, LLC under Contract No. DE-AC05-00OR22725 with the U.S. Department of Energy. The United States Government retains and the publisher, by accepting the article for publication, acknowledges that the United States Government retains a non-exclusive, paid-up, irrevocable, world-wide license to publish or reproduce the published form of this manuscript, or allow others to do so, for United States Government purposes. The Department of Energy will provide public access to these results of federally sponsored research in accordance with the DOE Public Access Plan (<http://energy.gov/downloads/doe-public-access-plan>).]*

## Low-cost scalable quartz crystal microbalance array for environmental sensing

Eric S. Muckley\*<sup>1,2</sup>, Cristain Anazagasty<sup>1</sup>, Christopher B. Jacobs<sup>1</sup>, Tibor Hianik<sup>3</sup>, Ilia N. Ivanov\*<sup>1</sup>

<sup>1</sup>Center for Nanophase Materials Sciences, Oak Ridge National Laboratory, Oak Ridge, TN 37831

<sup>2</sup>Bredesen Center for Energy Science and Engineering, University of Tennessee, Knoxville, TN 37996

<sup>3</sup>Faculty of Mathematics, Physics and Informatics, Comenius University, Mlynska dolina, 842 48 Bratislava, Slovakia

\*E-mail: muckleyes@ornl.gov, ivanovin@ornl.gov

### Abstract

Proliferation of environmental sensors for internet of things (IoT) applications has increased the need for low-cost platforms capable of accommodating multiple sensors. Quartz crystal microbalance (QCM) crystals coated with nanometer-thin sensor films are suitable for use in high-resolution (~1 ng) selective gas sensor applications. We demonstrate a scalable array for measuring frequency response of six QCM sensors controlled by low-cost Arduino microcontrollers and a USB multiplexer. Gas pulses and data acquisition were controlled by a LabVIEW user interface. We test the sensor array by measuring the frequency shift of crystals coated with different compositions of polymer composites based on poly(3,4-ethylenedioxythiophene):polystyrene sulfonate (PEDOT:PSS) while films are exposed to water vapor and oxygen inside a controlled environmental chamber. Our sensor array exhibits comparable performance to that of a commercial QCM system, while enabling high-throughput 6 QCM testing for under \$1,000. We use deep neural network structures to process sensor response and demonstrate that the QCM array is suitable for gas sensing, environmental monitoring, and electronic-nose applications.

### Introduction

Explosion of research and development efforts in the field of low-cost sensors is fueled by growth of the internet of things (IoT) paradigm in which environmental sensing and inter-device communication become omnipresent<sup>1</sup>. Efficient sensor integration into IoT networks is constrained by the limited scalability, portability, and versatility of traditional sensing platforms<sup>2</sup>. Size, weight, and power consumption requirements often restrict sensor deployment in autonomous vehicles and other IoT-compatible technologies. In addition, the performance of an individual sensor is often limited by its lack of selectivity and stability under changing ambient conditions<sup>3</sup>.

Selectivity, sensitivity, and scalability of distributed sensing networks are improved by combining individual sensors into local arrays<sup>4</sup>. Patterns in the responses of sensor arrays can be used for detection and identification of analytes

using statistical methods and machine learning techniques which mimic operation of biological olfactory systems, advancing technologies like the electronic nose (e-nose)<sup>3,5,6</sup>.

The quartz crystal microbalance (QCM) is a bulk acoustic wave sensor well-suited for deployment in sensing arrays for environmental, e-nose, and biomedical applications<sup>7,8</sup>. During QCM operation an electronic resonator drives thickness-shear mode oscillations of a piezoelectric quartz crystal while a frequency counter measures the crystal's resonance frequency, as depicted in Figure 1a. A QCM coated with a thin rigid film undergoes uniform mass loading resulting in a shift of resonance frequency ( $\Delta f$ ) given by the Sauerbrey equation

$$\Delta f = -\frac{2f_0^2}{A\sqrt{\rho_q\mu_q}}\Delta m,$$

where  $\Delta m$  is the change in mass of the film/crystal,  $f_0$  is the resonance frequency of the unloaded film/crystal, and  $A$ ,  $\rho_q$ , and  $\mu_q$  are the crystal's area, mass density, and shear modulus respectively<sup>9</sup>. Monitoring of  $\Delta f$  during mass loading/unloading events (gas sorption/desorption) allows estimation of  $\Delta m$  with sub-nanogram resolution<sup>10</sup>. Although its versatility allows the QCM to operate in vacuum, gaseous, and liquid environments, potential QCM applications are frequently limited by the high cost and large size of commercially-available platforms. Many commercial systems are capable of measuring frequency shift of only one crystal at a time, which restricts scalability of sensor networks and hinders high-throughput testing.

A versatile low-cost platform for building scalable QCM arrays is desirable for rapid sensor testing, environmental monitoring, and e-nose applications. Here we describe the design and applications of a portable gas sensor array based on open-source Arduino microcontrollers and OpenQCM electronic oscillator circuits. While multi-crystal commercial systems are typically sold for more than \$10,000, the QCM array described here is capable of simultaneous measurement of 6 crystals with a total cost of less than \$1,000 and a configuration suitable for expansion to a larger array size. To test performance of the array system, we measured the frequency shift of QCM crystals coated with the organic polymer composite based on poly(3,4-ethylenedioxythiophene):polystyrene sulfonate (PEDOT:PSS) and compare the crystal response with that of a 5 MHz QCM200 Stanford Research Systems (SRS). The structure of PEDOT:PSS consists of hydrophilic PSS used as an additive to enable aqueous solution processing of insoluble conducting PEDOT. While PEDOT:PSS is widely used as transparent electrode and hole extraction layer in organic optoelectronic devices<sup>11</sup>, its resistive water response also makes it suitable for application in flexible<sup>12</sup> and QCM-based relative humidity (RH)<sup>13</sup> and pressure sensors<sup>14</sup>. In order to test suitability of our array for sensing and e-nose applications, we coated crystals with PEDOT:PSS mixed with solutions of other functional organic materials including sulfonated copper phthalocyanine (CuPc), single wall carbon nanotubes (SWCNTs), and multi-wall carbon nanotubes (MWCNTs). We exposed the film-coated crystals to different water vapor and oxygen pressures and applied the resultant QCM data to a set of deep feedforward networks (DFNs), machine-learning tools which we use to identify the material deposited on each crystal and make predictions of H<sub>2</sub>O and O<sub>2</sub> pressure in the environmental chamber. Through this analysis we show that the low-cost 6-QCM array is capable of rapid high-throughput characterization of gas/vapor interaction with a wide range of functional organic composite films.

## Experiment

Design of the QCM array is shown in Figure 1b. Open-source Pierce oscillator boards were purchased from openQCM to drive oscillations of the QCM crystals. Open-source Arduino Micro microcontroller boards were used to supply power and record frequency output from each openQCM board. A 7-port externally-powered multiplexer was used to interface 6 Arduino/openQCM systems with a PC using a single USB cable. The electronics were packaged inside a protective box to enhance durability and portability of the system. A commercial 5 MHz SRS200 QCM controller was used as a reference for measuring performance of the open-source QCM system built here.

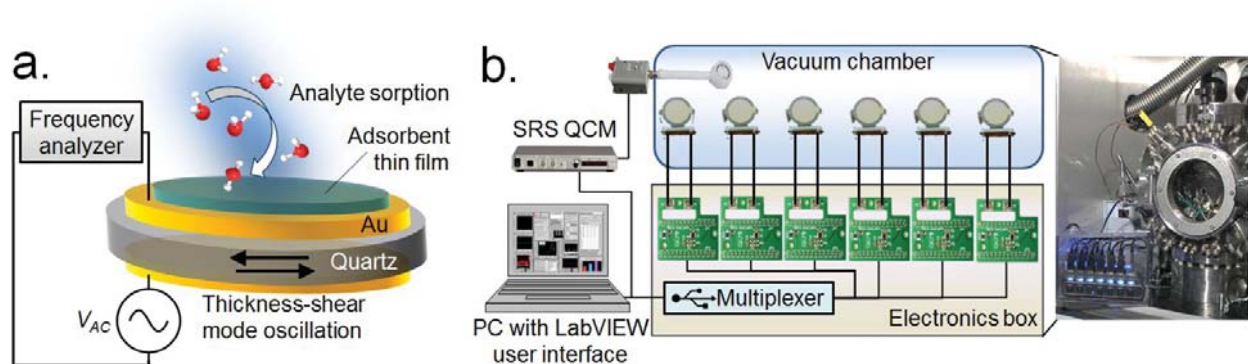


**Figure 1.** a. Schematic of QCM operation. Analyte sorption on film-coated QCM crystals causes a decrease in the resonance frequency of crystal's oscillations. b. Gas/vapor response of the QCM array was tested inside a vacuum chamber. Oscillator circuit boards, Arduino microcontrollers, and multiplexer were packaged inside a protective electronics box, seen in the bottom left corner of the image on the right. The QCM performance was referenced to that of a commercial SRS QCM system. All frequency measurements were recorded and displayed in real-time using a LabVIEW user interface on a PC.

Polished gold-coated 5 MHz AT-cut quartz crystals were purchased from International Crystal Manufacturing Co, Inc. Before film deposition, crystals were cleaned by ultrasonically in acetone for 30 minutes. PEDOT:PSS (ratios 1:6 and 3:4) and copper phthalocyanine-3,4',4'',4'''-tetrasulfonic acid tetrasodium salt (CuPc) were purchased from Sigma Aldrich. Semiconducting single wall carbon nanotubes (SWCNT) were purchased from Nanointegris Inc. Multi-wall carbon nanotubes were purchased from Cheap Tubes Inc. SWCNT were mixed with toluene, and MWCNT were mixed with dimethylformamide and dispersed by sonication for 30 minutes. For characterization of organic materials, PEDOT:PSS (3:4 ratio) was mixed with solutions of CuPc, SWCNTs, and MWCNTs, and 1  $\mu$ L of each mixed solution was deposited by drop casting on a QCM crystal. A 1  $\mu$ L drop of PEDOT:PSS (ratio 1:6) was also cast on a QCM crystal. For comparison with the SRS QCM system, single, double, and triple layers of PEDOT:PSS (3:4 ratio) were drop-cast on cleaned crystals. A single layer was cast on a crystal compatible with the SRS.

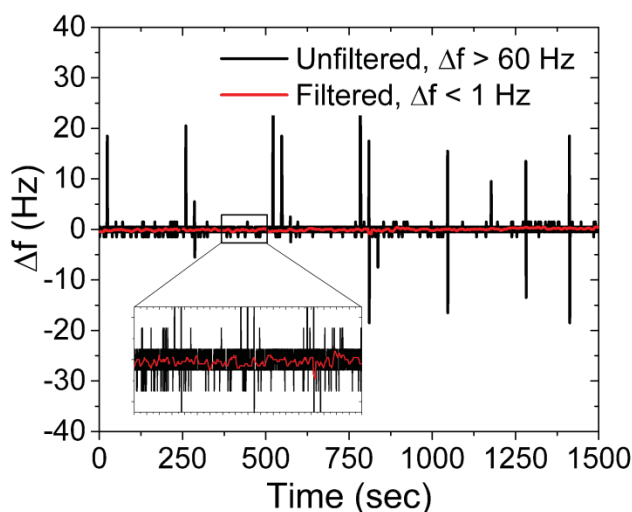


**Figure 2.** Comparison of noise in the QCM data stream with and without the digital median filter was implemented in LabVIEW. Under steady-state conditions, variance in the frequency shift  $\Delta f$  decreased from  $> 60$  Hz to  $< 1$  Hz upon application of the filter.

The film-coated and bare QCM crystals were mounted in a vacuum chamber prior to testing. Each QCM mount was connected to the electronics box outside the vacuum chamber using a 19-pin vacuum feed-through connector. Films were placed under vacuum of  $10^{-6}$  Torr for 3 hours in order to desorb contaminants and accommodate stress-related frequency drift of the QCM crystals. All measurements were performed at  $27 \pm 0.5^\circ\text{C}$  using a specially-designed environmental system<sup>15</sup>.  $\text{H}_2\text{O}$  vapor and  $\text{O}_2$  were released into the evacuated chamber using mass flow controllers (MFCs). The MFCs, SRS QCM, and Arduino-based QCM systems were all controlled using a LabVIEW-based custom user interface. During each experiment, an empty QCM crystal was measured as a control sample to monitor possible pressure response.

Originally, Arduino Mega prototyping boards were used to control the openQCM boards. These were replaced by Arduino Micro boards in order to reduce size and weight of the system. It was found that upon switching to the Arduino Micro boards the signal to noise ratio (SNR) of the QCM frequency response decreased by roughly a factor of 2. To improve SNR, a digital median filter with a sliding 5-point window was implemented in a custom data-processing section of the LabVIEW program. The filter receives frequency inputs from the microcontrollers, compares each value with the 2 preceding and 2 following values, and replaces the central value with the median of the 5 values. In this way, the median filter increased SNR by roughly a factor of 10 while preserving temporal resolution in the QCM data. A comparison of noise levels in the QCM data stream with and without the digital mean filter is shown in Figure 2.

## Results and Discussion

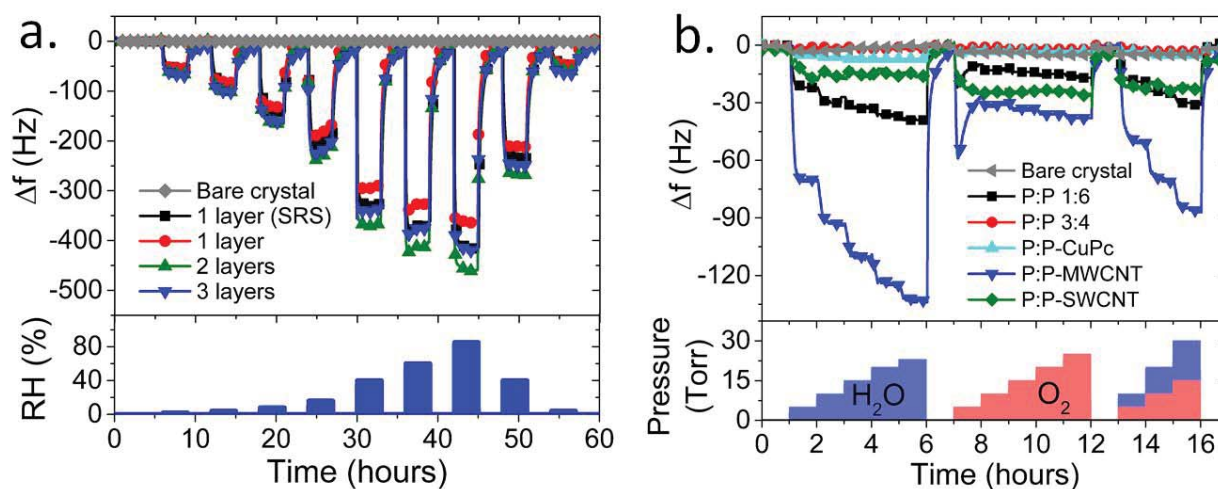


**Figure 3.** (a) Frequency shift ( $\Delta f$ ) of crystals coated with different layers of PEDOT:PSS (3:4 ratio) when exposed to varying levels of relative humidity (RH) (shown in lower panel). PEDOT:PSS-coated QCM crystal mounted in the QCM200 system (SRS) and a bare crystal were used as references. (b) Frequency shifts of QCMs coated with different organic materials in response to  $\text{H}_2\text{O}$ ,  $\text{O}_2$ , and an  $\text{H}_2\text{O}/\text{O}_2$  mixture. Gas/vapor pressures are shown in lower panel. Abbreviation key: P:P 1:6 = PEDOT:PSS (1:6 ratio); P:P 3:4 = PEDOT:PSS (3:4 ratio); P:P-CuPc = PEDOT:PSS (3:4 ratio) with copper phthalocyanine; P:P-SWCNT = PEDOT:PSS (3:4 ratio) with single-wall carbon nanotubes; P:P-MWCNT = PEDOT:PSS (3:4 ratio) with multi-wall carbon nanotubes.

The frequency shifts of QCM crystals coated with different numbers of PEDOT:PSS (3:4 ratio) layers are shown in Figure 3a under modulated RH environments. The frequency shifts of a bare crystal (shown in gray color) were used as a reference. In all crystals, the magnitude of  $\Delta f$  is proportional to the increase of RH. Response time, SNR, reversibility, and  $\Delta f$  response of the Arduino-based QCMs show good agreement with that of the SRS QCM, indicating that the performance of open-source system is comparable to that of the high-end commercial QCM. The

open-source 6-QCM array has advantages of high-throughput testing and the capability of increasing the number of sensors in the array for ~\$100 per each additional QCM. Its relatively small footprint makes the array suitable for a wider range of applications than most commercially-available systems.

To demonstrate potential applications of the QCM array, we coated 5 crystals with different functional organic materials and exposed them to changing concentrations of H<sub>2</sub>O and O<sub>2</sub>. The results are shown in Figure 3b. As expected, the frequency shifts show that most films undergo H<sub>2</sub>O/O<sub>2</sub> adsorption which is proportional to analyte pressure. The PEDOT:PSS-MWCNT composite exhibits the strongest adsorption of both H<sub>2</sub>O and O<sub>2</sub>, while the PEDOT:PSS-SWCNT composite exhibits a stronger frequency response to O<sub>2</sub> than to H<sub>2</sub>O. These findings are consistent with previous O<sub>2</sub>/H<sub>2</sub>O sorption measurements carried out on SWCNTs and MWCNTs<sup>16</sup>. The CuPc composite film shows insignificant O<sub>2</sub> adsorption, but some H<sub>2</sub>O adsorption. As expected, higher H<sub>2</sub>O adsorption occurs in the PEDOT:PSS 1:6 film than in the PEDOT:PSS 3:4 film due to the higher concentration of hydrophilic PSS.

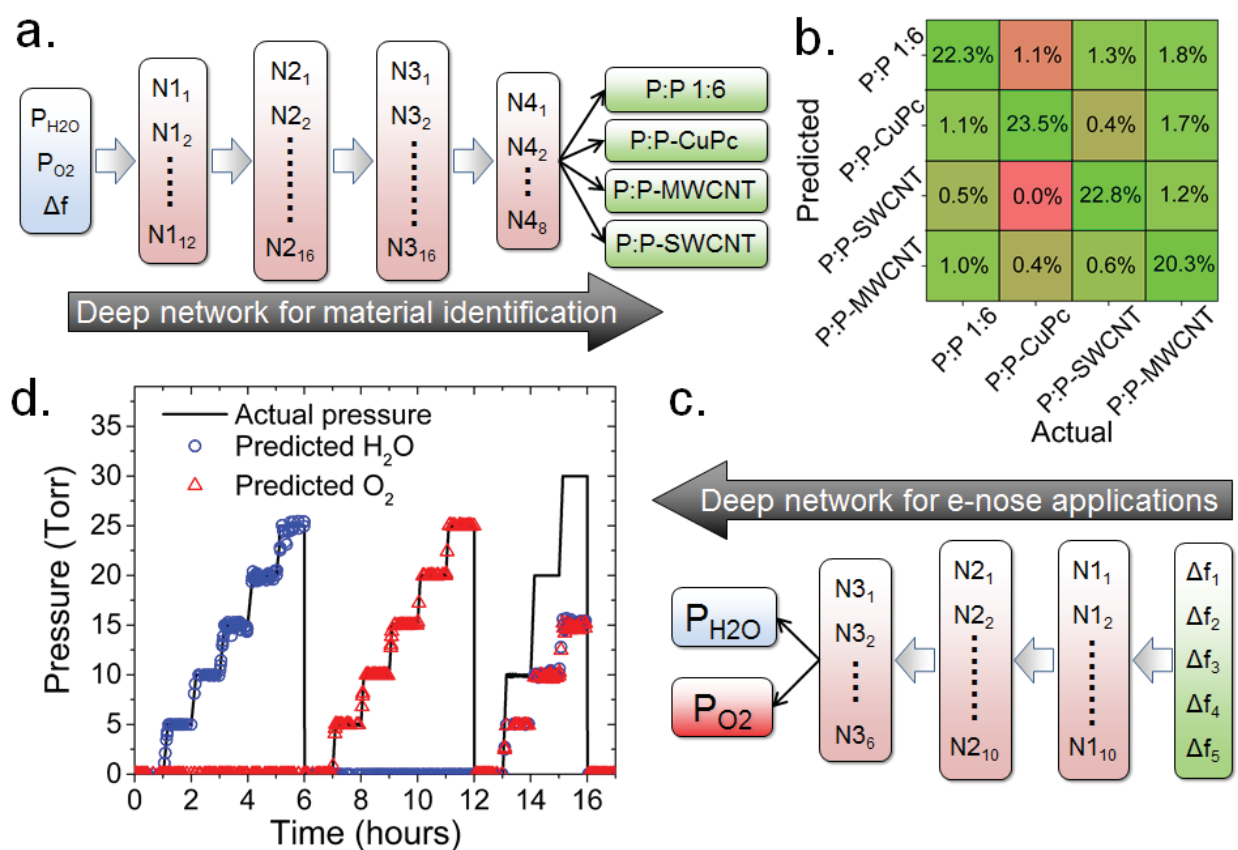


**Figure 4.** Deep feedforward neural network (DFN) used for classifying materials based on their frequency shift upon exposure to different concentrations of H<sub>2</sub>O and O<sub>2</sub>. b. Confusion matrix of classification results by the DFN in (a). c. DFN used for predicting H<sub>2</sub>O pressure (P<sub>H2O</sub>), and O<sub>2</sub> pressure (P<sub>O2</sub>) when frequency shifts of each film-coated crystal are used as inputs. d. Predictions made by the DFN in (c) for P<sub>H2O</sub> and P<sub>O2</sub>. The actual pressure sequence is shown in the bottom panel of Figure 3b. In the last sequence of gas/vapor steps, the DFN correctly predicts that the atmosphere is made of both H<sub>2</sub>O and O<sub>2</sub>, so the sum of the red and blue predictions results in approximation of the black line representing actual total pressure.

The results shown in Figure 3b were used as inputs in several deep feedforward neural networks (DFNs) to test suitability of the system for machine-learning analysis aimed at material classification and e-nose applications. The

first DFN was trained to identify the composition of thin films deposited on each QCM crystal. QCM frequency shift ( $\Delta f$ ),  $H_2O$  pressure ( $P_{H_2O}$ ), and  $O_2$  pressure ( $P_{O_2}$ ) were used as inputs in a 4-hidden layer network structure shown in Figure 4a. Each output class corresponds to one of the organic composite films: P:P 1:6, P:P-CuPc, P:P-MWCNT, and P:P-SWCNT. P:P 3:4 was not used because its corresponding  $\Delta f$  was close to that of a bare crystal. The FBN was implemented in Matlab using 30,185 samples of  $\Delta f$ ,  $P_{H_2O}$ , and  $P_{O_2}$ . 70% of the sample set was used for training, 15% for validation, and 15% for testing. Training was accomplished via scaled conjugate gradient decent. Results of classification predictions by the DFN are shown in the confusion matrix in Figure 4b. Each square corresponds to an instance when the actual material labeled on the bottom axis was predicted by the material labeled on the left axis. The percentages correspond to how many instances occurred in each prediction space out of the 4,528 test cases used for evaluation of the learning. The DFN achieves  $\sim 90\%$  accuracy in placing each of the films into its appropriate class. It is expected that the 10% classification error rate can be reduced by optimizing experimental conditions or DFN design. Results from the DFN demonstrate that the QCM array has the potential for use in applications involving material identification and classification.

We also tested suitability of the QCM array for e-nose applications. Using the frequency shift of 5 films as inputs in a 3-hidden layer DFN shown in Figure 4c, we predicted  $P_{H_2O}$  and  $P_{O_2}$  by training the DFN using Bayesian regularization. The FBN computations were implemented in Matlab using 30,185 samples of 5-dimensional  $\Delta f$  vectors. 70% of the sample set was used for training, 15% for validation, and 15% for testing. Results from DFN prediction tests are shown in Figure 4d. The actual pressure sequence is shown in the bottom panel of Figure 3b. The DFN achieves accurate predictions of  $P_{H_2O}$  and  $P_{O_2}$  with an average error of  $< 5\%$  during the entire gas/vapor pressure sequence. The average deviation between predicted and actual pressure was  $\sim 0.25$  Torr for  $P_{H_2O}$  and  $\sim 0.2$  Torr for  $P_{O_2}$ . While the DFN correctly distinguishes between the presence of  $H_2O$  and  $O_2$  in the first two staircase-like pressure sequences, it also identifies the region where both gas and vapor are present. During exposure to the mixed  $H_2O/O_2$  composition, DFN predictions for  $P_{H_2O}$  and  $P_{O_2}$  sum to the total pressure in the testing chamber, as expected. Results from the FDN analysis demonstrate the ability of the open-source QCM array to operate both as a platform for classification of organic sensing materials and as a flexible and scalable system for e-nose applications.

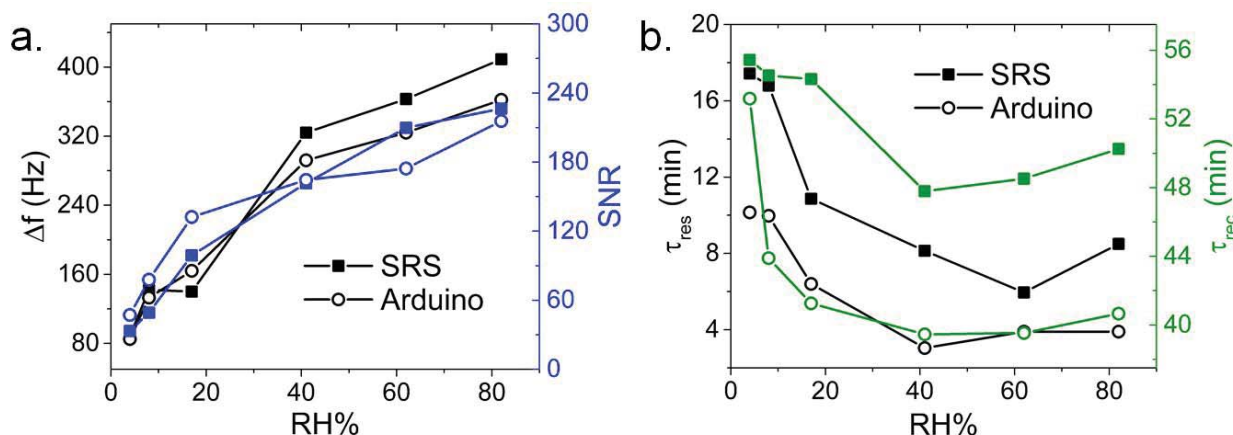


**Figure 5.** a. Comparison of  $\Delta f$  and SNR between Arduino-based QCM crystal coated with 1 layer of PEDOT:PSS 3:4 and SRS QCM crystal coated with the same film. b. Exponential time constants for response ( $\tau_{res}$ ) and recovery ( $\tau_{rec}$ ) of the same two crystals.

Finally, we performed a quantitative comparison between the Arduino-based QCM performance and the commercial SRS QCM using the  $H_2O$  pulses shown in Figure 3a. Figure 5 shows the magnitude of  $\Delta f$ , SNR, the time constant of the  $\Delta f$  response upon  $H_2O$  exposure ( $\tau_{res}$ ), and the time constant of the  $\Delta f$  recovery after purging of  $H_2O$  vapor ( $\tau_{rec}$ ). Both time constants were obtained by fitting the trace with the exponential fit. Response of the QCM crystal with one

layer of PEDOT:PSS 3:4 (open circles) is compared to the SRS crystal coated with the same film (solid squares). As shown in Figure 5a,  $\Delta f$  and SNR increase with RH and the difference in behavior between the Arduino-based and SRS QCMs is less than 10% for the 2-80% RH range. The time constants in Figure 5b show that the Arduino-based system exhibits faster response and recovery than the SRS at each RH level. At RH > 50%, the Arduino-based QCM achieves full response/recovery by up to 20% faster than the SRS. It is likely that the faster response times of the Arduino-based system are in part due to the crystal mount used for the SRS crystal, which may impede gas/vapor diffusion to the SRS crystal surface. In contrast, QCM mounts for the Arduino-based system (see Figure 1b) are open on both sides which allow for fast gas/vapor access to the sensor films.

## Conclusions

We designed, built, and tested an open-source platform for creating scalable QCM arrays based on Arduino microcontroller boards and openQCM Pierce oscillator circuits. Our system achieves less than a 10% difference in performance compared to a high-end commercial QCM system and improves the temporal QCM response. The total system costs under \$1,000 for simultaneous measurement of up to 6 QCM crystals, and new sensors can be added for ~\$100 per each additional sensor. By employing a set of deep neural networks for machine learning-assisted data analysis, we demonstrated that the Arduino-based QCM system is suitable for a range of diverse applications. These include high-throughput characterization of gas/vapor interaction with a variety of functional organic materials, material identification and classification, and environmental sensing applications. It is our hope that the low cost, portability, flexibility, and scalability of the system described here will foster greater utilization of QCM-related technologies in the growing IoT paradigm.

## Acknowledgement

The authors thank Vladimir Martis and Daryl Williams at Surface Measurement Systems Ltd.<sup>15</sup> for their support in developing the experimental design. The research was conducted at the Center for Nanophase Materials Sciences, which is a DOE Office of Science User Facility. CJ acknowledges financial support from ORNL Laboratory Directed Research and Development program. The sample of MWCNT was provided through user project CNMS2014-324. TH acknowledges funding from the European Union's Horizon 2020 research and innovation program under the Marie Skłodowska-Curie grant agreement No. 690898. This manuscript has been authored by UT-Battelle, LLC under Contract No. DE-AC05-00OR22725 with the U.S. Department of Energy.

## References

1. Gubbi, J., Buyya, R., Marusic, S. and Palaniswami, M., 2013. Internet of Things (IoT): A vision, architectural elements, and future directions. *Future Generation Computer Systems*, 29(7), pp.1645-1660. doi:10.1016/j.future.2013.01.010
2. Miorandi, D., Sicari, S., De Pellegrini, F. and Chlamtac, I., 2012. Internet of things: Vision, applications and research challenges. *Ad Hoc Networks*, 10(7), pp.1497-1516. doi:10.1016/j.adhoc.2012.02.016
3. Matzger, A.J., Lawrence, C.E., Grubbs, R.H. and Lewis, N.S., 2000. Combinatorial approaches to the synthesis of vapor detector arrays for use in an electronic nose. *Journal of combinatorial chemistry*, 2(4), pp.301-304. DOI: 10.1021/cc990056t
4. Star, A., Joshi, V., Skarupo, S., Thomas, D. and Gabriel, J.C.P., 2006. Gas sensor array based on metal-decorated carbon nanotubes. *The Journal of Physical Chemistry B*, 110(42), pp.21014-21020. DOI: 10.1021/jp064371z

5. Hong, H.K., Kwon, C.H., Kim, S.R., Yun, D.H., Lee, K. and Sung, Y.K., 2000. Portable electronic nose system with gas sensor array and artificial neural network. *Sensors and Actuators B: Chemical*, 66(1), pp.49-52. doi:10.1016/S0925-4005(99)00460-8
6. Gardner, J.W., Hines, E.L. and Wilkinson, M., 1990. Application of artificial neural networks to an electronic olfactory system. *Measurement Science and Technology*, 1(5), p.446. <http://dx.doi.org/10.1088/0957-0233/1/5/012>
7. Koshets, I.A., Kazantseva, Z.I., Shirshov, Y.M., Cherenok, S.A. and Kalchenko, V.I., 2005. Calixarene films as sensitive coatings for QCM-based gas sensors. *Sensors and Actuators B: Chemical*, 106(1), pp.177-181. doi:10.1016/j.snb.2004.05.054
8. Rodahl, M., Höök, F., Krozer, A., Brzezinski, P. and Kasemo, B., 1995. Quartz crystal microbalance setup for frequency and Q-factor measurements in gaseous and liquid environments. *Review of Scientific Instruments*, 66(7), pp.3924-3930. <http://dx.doi.org/10.1063/1.1145396>
9. Sauerbrey, G., 1959. Verwendung von Schwingquarzen zur Wägung dünner Schichten und zur Mikrowägung. *Zeitschrift für physik*, 155(2), pp.206-222. DOI: 10.1007 / BF01337937
10. Rodriguez-Pardo, L., Fariña, J., Gabrielli, C., Perrot, H. and Brendel, R., 2004. Resolution in quartz crystal oscillator circuits for high sensitivity microbalance sensors in damping media. *Sensors and Actuators B: Chemical*, 103(1), pp.318-324. doi:10.1016/j.snb.2004.04.060
11. Nardes, A.M., Kemerink, M., Janssen, R.A., Bastiaansen, J.A., Kiggen, N.M., Langeveld, B.M., van Breemen, A.J. and de Kok, M.M., 2007. Microscopic understanding of the anisotropic conductivity of PEDOT: PSS thin films. *Advanced Materials*, 19(9), pp.1196-1200. DOI: 10.1002/adma.200602575
12. Daoud, W.A., Xin, J.H. and Szeto, Y.S., 2005. Polyethylenedioxythiophene coatings for humidity, temperature and strain sensing polyamide fibers. *Sensors and Actuators B: Chemical*, 109(2), pp.329-333. doi:10.1016/j.snb.2004.12.067
13. Jaruwongrungrongsee, K., Sriprachuabwong, C., Sappat, A., Wisitsoraat, A., Phasukkit, P., Sangworasil, M. and Tuantranont, A., 2011, May. High-sensitivity humidity sensor utilizing PEDOT/PSS printed quartz crystal microbalance. In *Electrical Engineering/Electronics, Computer, Telecommunications and Information Technology (ECTI-CON), 2011 8th International Conference on* (pp. 66-69). IEEE. DOI:10.1109/ECTICON.2011.5947772
14. Muckley, E.S., Lynch, J., Kumar, R., Sumpter, B., Ivanov, I.N., 2016. PEDOT:PSS/QCM-based multimodal humidity and pressure sensor. *Sensors and Actuators B: Chemical*, 236 (pp. 91-98). doi:10.1016/j.snb.2016.05.054
15. Surface Measurement Systems UK Ltd. Unit 5, Wharfside Rosemont Road, Alperton London, HA0 4PE United Kingdom.
16. Muckley, E.S., Nelson, A.J., Jacobs, C.B. and Ivanov, I.N., 2016. Multimodal probing of oxygen and water interaction with metallic and semiconducting carbon nanotube networks under ultraviolet irradiation. *Journal of Photonics for Energy*, 6(2), pp.025506-025506. doi:10.1117/1.JPE.6.025506